Targeting host sialic acids in the upper respiratory tract with a broadly-acting neuraminidase to inhibit influenza virus transmission

Mila Brum Ortigoza[a,b,*], Catherina L. Mobini[b], Hedy L. Rocha[a], Stacey Bartlett[a], Cynthia A. Loomis[c], Jeffrey N. Weiser[b]

[a] Department of Medicine, Division of Infectious Diseases, New York University School of Medicine, New York, New York, USA

[b] Department of Microbiology, New York University School of Medicine, New York, New York, USA

[c] Department of Pathology, New York University School of Medicine, New York, New York, USA

* Address correspondence to Mila B. Ortigoza, mila.ortigoza@nyulangone.org

Abstract

The ongoing transmission of influenza A viruses (IAV) for the past 100 years continues to be a burden to humans. IAV binds terminal sialic acids (SA) of sugar molecules present within the glycocalyx of the upper respiratory tract (URT) in order to successfully gain entry and infect hosts. The two most common SA structures that are important for influenza virus infection and tropism are those with α2,3- and α2,6- linkages. These conformations are known to preferentially interact with avian and human viruses, respectively. While mice were previously thought to be an irrelevant system for studying IAV transmission due to their lack of α2,6-SA receptors in the trachea, we have successfully shown that transmission of influenza viruses in infant mice is highly efficient, suggesting the presence of these receptors in the URT, a site never previously explored. In this study, we mapped the SA composition of the URT of mice using *in situ* immunofluorescence and examined their contribution to transmission among infant mice. We demonstrate that mice express both α2,3- and α2,6-SA in the URT and that the difference in expression between infants and adults may contribute to the variable transmission phenotype. Furthermore, we found that by selectively blocking α2,3- or α2,6-SA receptors within the URT of infants using lectins was necessary but insufficient to inhibit transmission, and simultaneous blockade of both receptors was essential. Using a broadly-acting neuraminidase (ba-NA) to indiscriminately remove both types of SA *in vivo* successfully inhibited viral shedding and prevented transmission of various influenza virus strains. These findings suggest that broadly targeting host SA may be an effective approach to inhibit IAV transmission.

Importance

The ability of influenza viruses to jump species and infect humans from animal reservoirs continues to pose a significant pandemic threat. Previous research investigating influenza virus transmission has primarily focused on viral mutations that alter host receptor binding specificity and facilitate virus entry. However, this study takes a different approach by investigating the role of influenza virus receptors *in vivo* and their role in viral replication, shedding, and transmission. Our findings challenge the notion that α2,6-SA expression is a key factor in transmission efficiency in humans, as viruses that can engage more than one SA conformation can still transmit. Our study provides evidence that neuraminidases with broad activity, capable of removing both α2,3- and α2,6-SA *in vivo*, can target host factors critical for transmission. Therefore, these broadly-acting neuraminidases have the potential to be the next generation of antivirals capable of preventing the spread of respiratory pathogens that rely on SA for infection.

Introduction

Respiratory pathogens adapt to the host environment to ensure their survival, and the most successful ones are those that become endemic in a population by spreading from one host to another without causing fatal illness. Influenza viruses have caused several pandemics over the past century and remain prevalent in humans. Current measures such as vaccines and antivirals to limit intra-host transmission have proven ineffective due to low vaccination coverage, limited antiviral use, and the rapid emergence of new viral strains through antigenic drift that evade immune defenses. Therefore, there is an urgent need to understand the biology influenza virus transmission and devise improved strategies to disrupt its transmission cycle.

Although mice are not the natural hosts for influenza viruses, they can still be infected through intranasal inoculation, and have become a valuable tool for studying influenza virus biology (1-3). However, mouse-to-mouse transmission has historically been inefficient and inconsistent, leading researchers to dismiss mice as a useful model for studying influenza virus transmission (1, 4-9). This was largely due to the absence of α2,6- sialic acid (SA) receptors in the murine trachea, which are known to bind and release IAV strains that are significant to humans.

It is known that avian influenza viruses (AIV) preferentially bind to α2,3-SA glycosidic linkage, which is expressed in the intestine of birds and is a site of viral replication. However, recent studies have shown that the tracheal epithelium of birds also express both α2,3-SA and α2,6-SA, indicating a broader distribution of influenza virus receptors in birds than previously known (10). This raises the possibility that birds may serve as both the reservoir and spillover for influenza viruses into humans, similar to swine (11). In contrast, humans predominantly express α2,6-SA in the upper respiratory tract (URT), where initial infection, viral replication, and shedding occur. Influenza viruses that preferentially bind to α2,6-SA are more efficient at human-to-human transmission. While α2,6-SA is found in parts of the lower respiratory tract (LRT) such as the trachea, bronchi, and bronchioles, it is absent in alveolar cells. On the other hand, α2,3-SA is mainly present in the LRT, particularly in alveolar cells, but can also be found in specific cells of the URT (12).

Studies evaluating the composition of α2,3-SA and α2,6-SA receptors in the respiratory tract of mice have been limited to LRT-derived cells and tissues. In *ex vivo* murine tracheal epithelial cultures (mTEC), only α2,3-SA was detected (13), while in murine lungs, both α2,3-SA and α2,6-SA were present (14, 15). However, the composition of these receptors in the murine URT (nose, pharynx, larynx), the anatomical region where virus is first acquired and shed, has not been evaluated.

Additionally, despite suggestions that α2,6-SA may not be necessary for human influenza virus infection and replication (14), its direct role in transmission has not been assessed.

We learned from our previous work that, in contrast to adult mice, infant mice support efficient transmission of influenza viruses among littermates in an age-dependent and strain-dependent fashion (9). We also demonstrated that co-infection with *S.pneumoniae* reduced the efficiency of IAV transmission through the activity of bacterial nanA, a neuraminidase known to remove both α2,3- and α2,6-SA, and not nanB, a neuraminidase known to remove only α2,3-SA. This suggested that α2,6-SA are indeed present and functional in the URT of infant mice.

Thus far, we learned that there are three key bottlenecks determining transmission in mice, which can be categorized into three main stages: virus replication in the URT of the infected (index) host (stage 1), elution of virus from the URT (shedding) of the infected host (stage 2), and arrival of virus in the URT of uninfected (contact) hosts and establishment of productive infection (stage 3), (**Figure 1**). If there is an imbalance between the index's ability to replicate and shed virus and the contact's ability to acquire infection, transmission will be interrupted. Hence, successful inhibition of transmission requires designing vaccines and therapeutics that can decrease viral shedding and/or block viral acquisition. To achieve this, we naturally directed our *in vivo* studies to the URT, which is the initial site of contact between the virus and host, in order to understand the differences in the SA receptor repertoire and distribution *in vivo* of both adult and infant mice. We then examined how manipulating these receptors could reveal their specific roles in virus shedding and transmission.

FIGURE 1

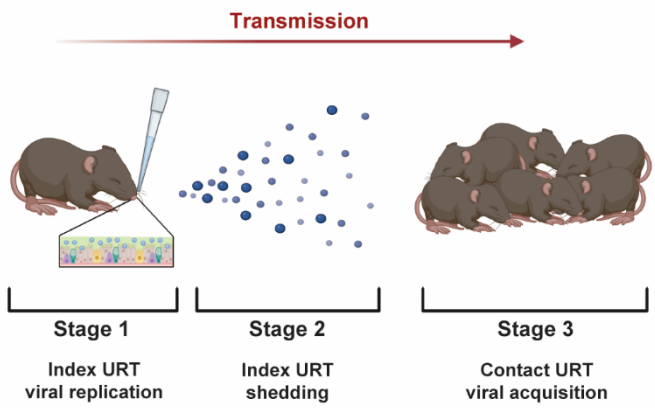

Figure 1. Stages of Transmission.
The transmission of influenza virus from index to contact mice involves three distinct stages. First, the virus replicates in the upper respiratory tract (URT) of the infected index mice (**stage 1**). Next, the virus is expelled into the environment (**stage 2**). Finally, virus is acquired by uninfected contact mice and infection is established in the URT (**stage 3**).

RESULTS

Infant and adult mice express both α2,3 and α2,6 sialic acids in the upper respiratory tract.

Successful transmission of IAV in mice was previously determined to be more efficient in younger mice than older mice (9). Building upon this knowledge, we sought to evaluate which stage of transmission was most deficient in adult mice compared to infants. To achieve this, we conducted infection experiments using a low-volume intranasal (IN) inoculum in both adult and infant C57BL/6J mice in order to restrict the infection to the URT (7, 16). Infants were inoculated with a 3µl volume, while adults received a slightly higher 6µl volume. The IAV strain used was A/X-31 (H3N2), with infants receiving 300 plaque-forming units (PFU) and adults receiving 10^5 PFU. After infection, the index mice were placed back in the cage with naïve contacts at a ratio of approximately 1 index to 2-3 contact mice. To collect samples for virus shedding analysis, the nares of each mouse were gently dipped in viral medium on a daily basis. Transmission was evaluated in the contact mice by measuring the virus present in retrograde URT lavage samples taken at 4 days post-infection (dpi) (**Figure 2A**). It is worth noting that previous findings from our research have demonstrated that transmission to contact mice reaches over 90% by 4dpi. At 4 dpi, the URT replication of A/X-31 in adults (stage 1) was found to be comparable to that in infants (**Fig.2B-left**). However, intriguingly, during stage 2, which encompasses the overall shedding kinetics from days 1 to 4, infants exhibited higher levels of index shedding compared to adults. This difference was particularly pronounced during the initial two days when peak shedding is expected (17), $p<0.001$ (**Fig.2B-middle**). Furthermore, when it came to the transmission of A/X-31 to uninfected contact mice (stage 3), infants displayed a higher efficiency with a transmission rate of 92%, in contrast to adults with a rate of 33%, $p<0.0001$ (**Fig.2B-right**). Additionally, the median URT titers in the contact animals at 4 dpi exhibited a significant difference between infants and adults, $p<0.0001$. Collectively, these data suggest that while URT replication was similar between infants and adults, there were notable disparities in shedding (stage 2) and the acquisition of the virus by contact mice (stage 3) in adults. This observation prompted us to explore the host factors within the epithelium interphase that might play a role in this distinct shedding phenotype. Specifically, our attention turned towards investigating the role of surface sialic acids in shedding.

To explore the potential differences in SA levels and their distribution in the URT between infant and adult mice, we aimed to determine if these variations could explain the discrepancies in transmission efficiencies. Our investigation involved assessing the presence and distribution of α2,3-SA and α2,6-SA receptors in the URT through histological sections of the murine nasopharynx from

naïve C57BL/6J mice. For this purpose, we utilized specific lectins that prefer binding to either α2,3-SA (*maackia amurensis* lectin, MAL) or α2,6-SA (*sambucus nigra* lectin, SNL). Additionally, we employed *erythrina crystagalli* lectin (ECL), which binds to underlying β-galactose after desialylation. These lectins were applied to paraffin-embedded coronal sections of the heads from both 5-day-old infant mice and 8-week-old adult mice. The *in situ* immunohistochemical (IHC) staining of these sections revealed the presence of α2,3-SA and α2,6-SA receptors in the olfactory and respiratory epithelium of the URT in both infants and adults (**Fig.2C**). The signal for desialylated β-galactose (ECL) was minimal. Interestingly, the expression of α2,6-SA in the respiratory epithelium of infants appeared to be associated with the location of mucus-secreting cells, as indicated by the Alcian Blue/PAS stained sections (**Fig.2C-d, arrows**).

We also examined the distribution of α2,3-SA and α2,6-SA receptors in the LRT of both infants and adults (**Supl. Fig1**). Similar to the findings in the URT, we observed abundant expression of both α2,3-SA and α2,6-SA receptors in the lungs of both infants and adults, which aligns with previous reports (14). In contrast, when we assessed tracheal sections from both infants and adults, we detected the presence of only α2,3-SA receptors. This finding is consistent with prior *ex-vivo* studies conducted on mTECs and previous histological evaluations (13, 14). It is worth noting that the absence of a signal from the α2,6-binding lectin SNL in the trachea suggests that, under the experimental conditions used, cross-reactivity or low affinity binding of SNL to α2,3-SA is unlikely.

Lastly, we conducted immunoblotting and IHC to quantify the levels of α2,3-SA and α2,6-SA in the URT of infants and adults. URT secretions were collected via retrograde URT lavage after sacrifice, and biotinylated lectins were used for SA detection. The results showed that the URT secretions of adult mice had lower overall sialylation compared to those of infants (**Fig.2D**). Consistently, *in situ* IHC analysis using lectin staining revealed a lower immunofluorescence (IF) signal intensity in the URT of adults compared to infants (**Fig.2E**). These findings indicate that both infants and adults express the necessary SA residues that are important for influenza virus infection, replication, and transmission. However, infants exhibit higher levels of sialylated receptors relative to their size. It is interesting to note that even though the expression of sialylated receptors in the URT of adult mice is relatively lower, it is still sufficient to support viral infection and replication following experimental IN inoculation. However, it appears that the number of receptors distributed in the URT of adults seems to be inadequate for efficient viral shedding and establishing *de novo* infection through natural transmission to contact mice. This suggests that the scarcity of SA receptors in adult mice may contribute, at least in part, to the observed inefficient transmission phenotype in this cohort.

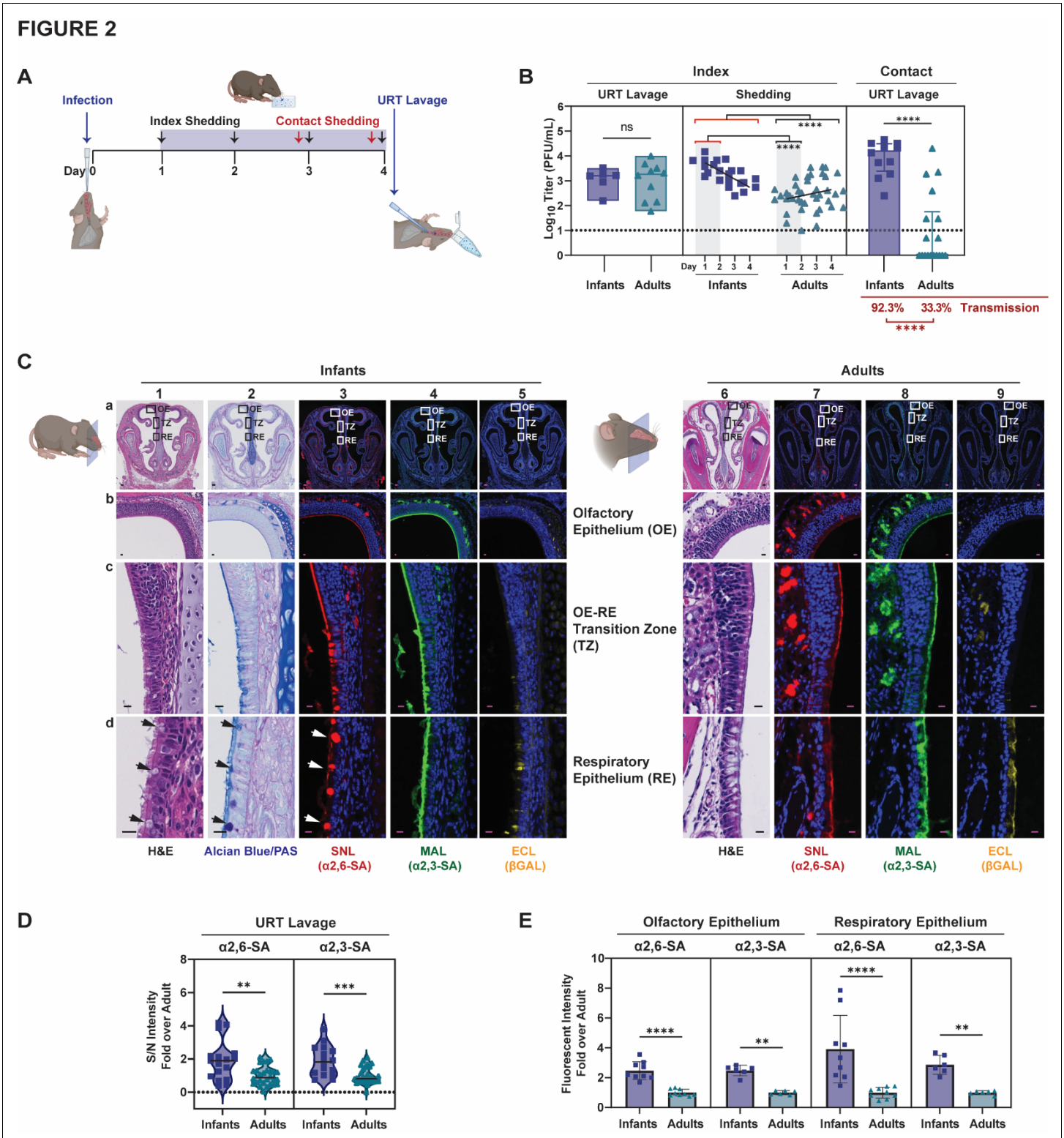

Figure 2. Differential Expression of Sialic Acid in the URT of Mice.

A. Schematic of Influenza virus transmission. At day 0, index pups were infected IN with A/X-31 (infants at 300 PFU, adults at 10^5 PFU) and cohoused with uninfected littermates (contact) for 4 days prior to being evaluated for transmission via retrograde URT lavage after sacrifice. Shedding was collected on days 1-4 for index and days 3-4 for contacts by dipping the nostril of each pup into viral media daily and assessing for infectious virus via plaque assay. **B.** Transmission of A/X31 in infant (blue) and adult (green) mice. Viral titers of lavage fluid and shed secretions were

evaluated via plaque assay. Each symbol represents the titer measured from a single mouse, with median values indicated by a line. **C.** Immunohistochemistry of uninfected infants and adult mice nasopharynx. After sacrifice, heads were fixed with 4% paraformaldehyde, paraffin embedded, sectioned through the nasopharynx, and stained with conjugated lectins. Zoomed-in images of the boxed inserts are represented by rows b, c, and d. **D.** Uninfected infant and adult mice were subjected to retrograde URT lavage, and fluid was immunostained with biotinylated lectins to assess for sialylation. Signals were normalized to membrane background. Median is denoted by a line. **E.** Fluorescent signal from immunohistochemistry (in C) was assessed using ImageJ. Signals for each epithelial compartment was obtained in 5 random locations of at least 2-3 individual mice. Values were normalized to size of the head, and fold induction was calculated over the adult mice average signal. Bars represent median ± interquartile range. **All panels**: Differences among two group medians were analyzed using the Mann-Whitney test. Experiments represent at least 2 biological replicates. Infant mice were 4-7 day old; Adult mice were 8 week-old; * ($p < 0.05$), ** ($p < 0.01$), *** ($p < 0.001$), **** ($p < 0.001$). Red brackets in statistical comparisons represent the reference group. URT, upper respiratory tract; PFU, plaque-forming unit; H&E, hematoxylin and eosin stain; AB/PAS, alcian blue and periodic acid-Schiff stain; SNL, *sambucus nigra* lectin; MAL, *maackia amurensis* lectin; ECL, *erythrina crystagalli* lectin; S/N, signal-to-noise ratio; Dotted line denotes limit of detection (10 PFU/mL), where indicated; Zero values were set to 1 PFU/mL.

Therapeutic blockade of both α2,3 and α2,6 sialic acids is required to inhibit influenza virus transmission.

To evaluate the functional capacity of α2,3-SA and α2,6-SA receptors expressed in the URT of mice *in vivo*, we used the infant mouse model of influenza virus transmission (9). Infection of infant index pups in a litter (3-5 days of age) was performed with low-volume IN inoculum (3µl) using 300 PFUs of IAV strain A/X-31 (H3N2), as previously described. Both index and contact pups were subsequently treated twice a day (BID) with unconjugated lectins IN for four days, with the first treatment starting at ~6 hours post-infection (hpi). Virus shedding was collected daily by gently dipping the nares of each pup in viral medium, and transmission within the litter was assessed by measuring virus levels in retrograde URT lavages at 4 dpi (**Fig.3A**).

We observed notable inhibition of transmission in all lectin-treated groups in a dose-dependent manner, with simultaneous blockade of α2,3-SA and α2,6-SA receptors being more effective in inhibiting transmission compared to blocking individual receptors alone (**Fig.3B**). Interestingly, when blocking α2,6-SA alone with higher concentrations of SNL, the transmission of A/X-31 was more effectively inhibited than when blocking α2,3-SA alone. These findings align with *in vitro* studies using solid-phase glycan binding assays, which demonstrate that the A/X-31 virus prefers binding to α2,6-SA receptors over α2,3-SA receptors, although it can bind to both receptors (18-21). Overall, these

results indicate that functional α2,3-SA and α2,6-SA receptors are present in the URT of infant mice and play a crucial role as host factors contributing to the transmission of A/X-31 in this model.

To determine the impact of SA receptor blockade on different stages of transmission, we examined each stage separately using the mid-range dose of 4mg/Kg/day of lectin treatment. In stage 1, which involves URT viral replication in the index mice, blocking either α2,3-SA or α2,6-SA receptor alone or simultaneously did not affect viral replication (**Fig.3C-left**). In stage 2, where index shedding is assessed, the overall shedding titers during the 1-4-day period were similar between mock-infected infants and those with single receptor blockade (α2,3-SA or α2,6-SA), as well as double receptor blockade (**Fig.3C-middle**). However, during the critical first two days when peak shedding typically occurs (days 1-2), there was a statistically significant decrease in shedding only when both α2,3-SA and α2,6-SA receptors were simultaneously blocked. This suggests that effective shedding of the virus from the URT may require the availability of SA receptors. Finally, in stage 3, which focuses on viral acquisition in contact pups, blocking α2,6-SA receptor alone or in combination with α2,3-SA blockade had the most significant impact. This resulted in a transmission efficiency of 38.7% and 42.9%, respectively, compared to 75% in the mock-treated pups (**Fig.3C-right**). These findings indicate that the transmission of A/X-31 to contact pups is predominantly dependent on the availability of α2,6-SA receptors in the recipients, as previously suggested (9).

To investigate the role of α2,6-SA in the transmission of A/X-31, we utilized mice lacking the gene *st6gal1* (*st6gal1*-KO) which lack the enzyme β-galactoside α2,6-sialotransferase 1 (ST6GAL1) (22). This enzyme catalyzes the addition of α2,6-SA to terminal β-galactose of glycoproteins and glycolipids present in the URT and mucosal surfaces. Hence, the *st6gal1*-KO mice are not expected to contain terminal α2,6-SA on the surface of glycoconjugates in the respiratory tract (14). Immunohistochemistry confirmed the absence of α2,6-SA expression throughout the URT of *st6gal1*-KO infant mice (**Suppl. Fig2**). Surprisingly, transmission efficiency of A/X-31 in *st6gal1*-KO was comparable to that in wild-type C57BL/6J (WT) mice (**Fig 3D**). To investigate whether residual α2,3-SA expression in the URT contributed to the observed transmission phenotype, we conducted additional experiments by blocking α2,3-SA in combination with the absence of α2,6-SA. We found that complementing receptor blockade *in trans* in the *st6gal1*-KO pups, peak index viral shedding on day 1-2 and viral acquisition in the contact pups were inhibited. These findings support our previous observation that simultaneous targeting of α2,3-SA and α2,6-SA is necessary for effective inhibition of transmission, particularly when both stage 2 (shedding by index) and stage 3 (acquisition by contacts) of the transmission route are targeted. Moreover, these results indicate that the α2,6-SA linkage created by the ST6GAL1 enzyme is dispensable, as suggested in previous studies (14, 23), and

suggest that some influenza viruses may exhibit broader receptor preferences in vivo than previously assumed.

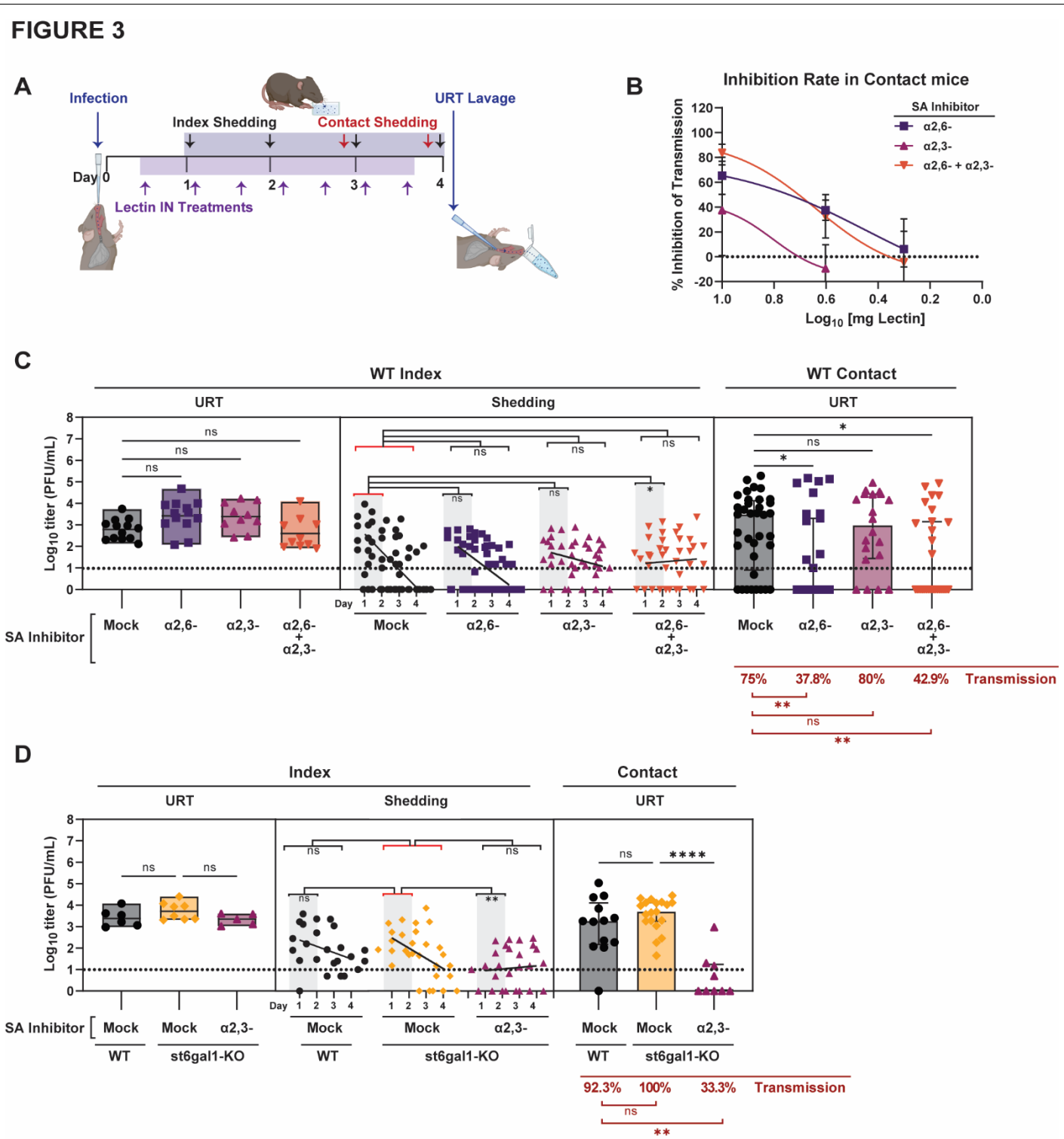

Figure 3. Therapeutic blockade of both α2,3 and α2,6-SA is required to inhibit influenza virus transmission.

A. Schematic of lectin treatment to block influenza virus transmission. At day 0, pups were infected IN with 300 PFU of A/X-31 (index) and cohoused with uninfected littermates (contact) for 4 days prior to being evaluated for transmission via retrograde URT lavage after sacrifice. Shedding was collected on days 1-4 for index and days 3-4 for contacts by

dipping the nostril of each pup into viral media and assessing for infectious virus via plaque assay. IN lectin treatment was given to both index and contacts, and started 6 hpi and continued twice daily until end of experiment. **B.** Transmission inhibition rate in contact mice represented as percent (%) inhibition over decreasing lectin (inhibitor) concentration. % Inhibition was calculated using the following formula: y=100*(1-(y/71.9)), where 71.9 is the average transmission rate of mock-treated litters. Mean transmission is plotted with error bars representing the standard error of the mean. **C.** Transmission blockade by lectin inhibitor is represented by virus titers plotted at each stage of transmission. Left panel (stage 1, index URT replication), middle panel (stage 2, index shedding), right panel (stage 3, contact acquisition). **D.** Transmission assay in WT and *st6gal1*-KO infants with or without α2,3-SA inhibitor (MAL) blockade. **All panels**: Median is denoted by a line. within box plots and bar graphs ± interquartile range. Simple linear regression was plotted in shedding panels. Differences among multiple group medians were analyzed using the Kruskal-Wallis test. Experiments represent at least 2 biological replicates. Transmission rates were calculated using Fisher's Exact test. Infant mice were 4-7 day old; * ($p < 0.05$), ** ($p < 0.01$), *** ($p < 0.001$), **** ($p < 0.001$). Red brackets in statistical comparisons represent the reference group. URT, upper respiratory tract; PFU, plaque-forming unit; IN, intranasal; Mock group represents the vehicle-treated (placebo) group. Dotted line denotes limit of detection (10 PFU/mL), where indicated; Zero values were set to 1 PFU/mL.

Simultaneous α2,3- and α2,6- desialylation with broadly-acting neuraminidase inhibits influenza virus transmission *in vivo*.

To confirm the effectiveness of depleting both α2,3-SA and α2,6-SA in inhibiting the transmission of influenza A/X-31 in mice, a broadly-acting neuraminidase (ba-NA), DAS181, was utilized. DAS181 is a recombinant bacterial NA which expresses the NA catalytic domain derived from *Actinomyces viscosus* fused with an epithelium-anchoring domain derived from the human protein amphiregulin (24), and it is currently being tested in clinical trials for its ability to reduce parainfluenza pneumonia in immunocompromised patients (25). DAS181 targets and removes both α2,3-SA and α2,6-SA. This is in contrast to zanamivir, an FDA-approved drug, which targets the viral NA and prevents the desialylation of host surface SA.

To evaluate the *in vivo* desialylation effect of ba-NA, the amount of desialylated glycoconjugates in the URT of infected pups was quantified using *in situ* IHC and immunoblots of URT lavage. Naïve pups were either infected with A/X-31 or treated with ba-NA DAS181 (0.5 mg/Kg) via IN administration for 2 days before sacrifice. URT desialylation was assessed by *in situ* IHC via lectin staining (**Fig.4A**). Only pups infected with A/X-31 showed detectable signals for IAV nucleoprotein (NP) in the olfactory and respiratory epithelium (**Fig.4A_2,5,8 and Fig.4B**). As expected, both A/X31 infected or ba-NA treated pups exhibited increased IF signal intensity for

desialylated β-galactose sugars, suggesting that a ba-NA treatment was as effective as IAV infection in desialylating the URT of pups (**Fig.4A_3,6,9 and Fig.4B**). Moreover, URT secretions from A/X-31-infected or ba-NA-treated pups were collected by retrograde URT lavages after sacrifice and immunostained with biotinylated ECL. As expected, desialylated β-galactose sugars were more abundant in the secretions of A/X-31-infected or ba-NA-treated pups compared to secretions from mock-treated animals (**Fig.4C**).

The therapeutic potential of *in vivo* desialylation on transmission was assessed in the infant mouse model. URT infection with A/X-31 was performed on index pups in a litter as previously described. Both index and naïve contact pups were then treated daily IN with ba-NA DAS181 or the neuraminidase inhibitor (NA-I), zanamivir for 4 days, with the first treatment starting at 2 hpi. Daily collection of virus shedding and evaluation of intralitter transmission in contact littermates were performed by measuring virus levels in retrograde URT lavages at 4 dpi (**Fig.5A**). The inhibition of A/X-31 transmission was observed in a dose-dependent manner for both ba-NA and NA-I (**Fig.5B**).

To determine the therapeutic window of ba-NA, the inhibition of transmission was evaluated when pups were treated at different time points after infection. Index pups in a litter were infected IN with A/X31 as previously described. Subsequently, both index and naïve contact pups were treated daily IN with ba-NA or NA-I. The first cohort received treatment starting at 2 hpi, the second cohort at 24 hpi, the third cohort at 48 hpi, and the fourth cohort at 72 hpi. Transmission was assessed in contact littermates by measuring virus levels in retrograde URT lavages at 4 dpi. Transmission inhibition by ba-NA was 100%, 86.7%, 35.8%, and 27.3% when treatment was initiated at 2, 24, 48, and 72 hpi, respectively (**Fig.5C**). NA-I exhibited a similar transmission inhibition profile to ba-NA, with rates of 89.7%, 74.3%, 35.9%, and 29.5% when administered at 2, 24, 48, and 72 hpi, respectively. We next evaluated the effects of delayed ba-NA treatment in each stage of transmission. Regarding URT viral replication in the inoculated index (stage 1), delayed treatment with ba-NA had no significant impact (**Fig.5D-left**). In stage 2, viral shedding was reduced only when treatment with ba-NA treatment was initiated early after infection, specifically prior to 24 hours (**Fig.5D-middle**). Lastly, ba-NA was effective in preventing viral transmission to contacts (stage 3) by >40% if administered within 48 hr of exposure to the infected index (**Fig.5D-right**). Overall, these findings indicate that the efficacy of ba-NA treatment in preventing viral transmission decreases with longer delays in initiating the therapy.

To determine which cohort had the most influence on influenza virus transmission, we conducted separate treatments using ba-NA on either the index pups, the contact pups, or both the

index and contact pups, and analyzed each transmission stage individually. Compared to mock, URT viral replication in the infected index (stage 1) was unaffected by any of the treatment combinations (**Fig.5E-left**). Interestingly, overall shedding (stage 2) was reduced when the index pups received ba-NA treatment (**Fig.5E-middle**), consistent with our prior observation that dual receptor blockade with lectins resulted in reduced shedding (**Fig.3C-middle**). This confirms the importance of SA availability in the URT of the index in viral shedding. Furthermore, viral acquisition in the contact pups (stage 3) was significantly inhibited when either the index, the contact, or both the index and contact were targeted for URT desialylation, resulting in transmission efficiencies of 10.5%, 6.3%, and 0%, respectively (**Fig.5E-right**). This suggests that desialylation of both α2,3-SA and α2,6-SA is more effective in inhibiting IAV shedding, and transmission compared to exogenous receptor blockade. Additionally, it indicates that the mechanism of transmission inhibition by ba-NA involves both reducing shedding from the infected index and protecting naïve contacts from acquiring the virus (prophylaxis).

Depletion of influenza virus receptors in the contacts was expected to prevent acquisition of infection through transmission. However, it was surprising to observe that the depletion of SA receptors in the URT had an additional effect on reducing shedding by the index, even though viral release from the URT surface is not known to require the continuous presence of sialylated glycoconjugates. In contrast, it is known that the removal of terminal SA by viral NA promotes viral elution (26). To investigate if the presence of SA and its interaction with the virus during egress is an important requirement for shedding from the URT, we targeted host SA using ba-NA at different concentrations and assessed shedding and transmission of A/X31. Increasing the dose of ba-NA resulted in a corresponding decrease in overall shedding dynamics, peak shedding (days 1-2), and viral acquisition in contacts in a dose-dependent manner (**Fig 5F-left**). Furthermore, to determine if the dissociation of the virus from SA is crucial for shedding, we inhibited the ability of viral NA to cleave SA using NA-I at various concentrations and assessed shedding and transmission. As the dose of NA-I increased, the overall shedding dynamics did not show significant changes compared to the mock group, but both peak shedding (days 1-2) and transmission decreased correspondingly (**Fig 5F-right**). Collectively, these findings suggest that the mechanism of viral shedding in vivo from the URT is partially dependent on the presence of surface SA and its interaction with the virus, followed by its dissociation from the virus.

FIGURE 4

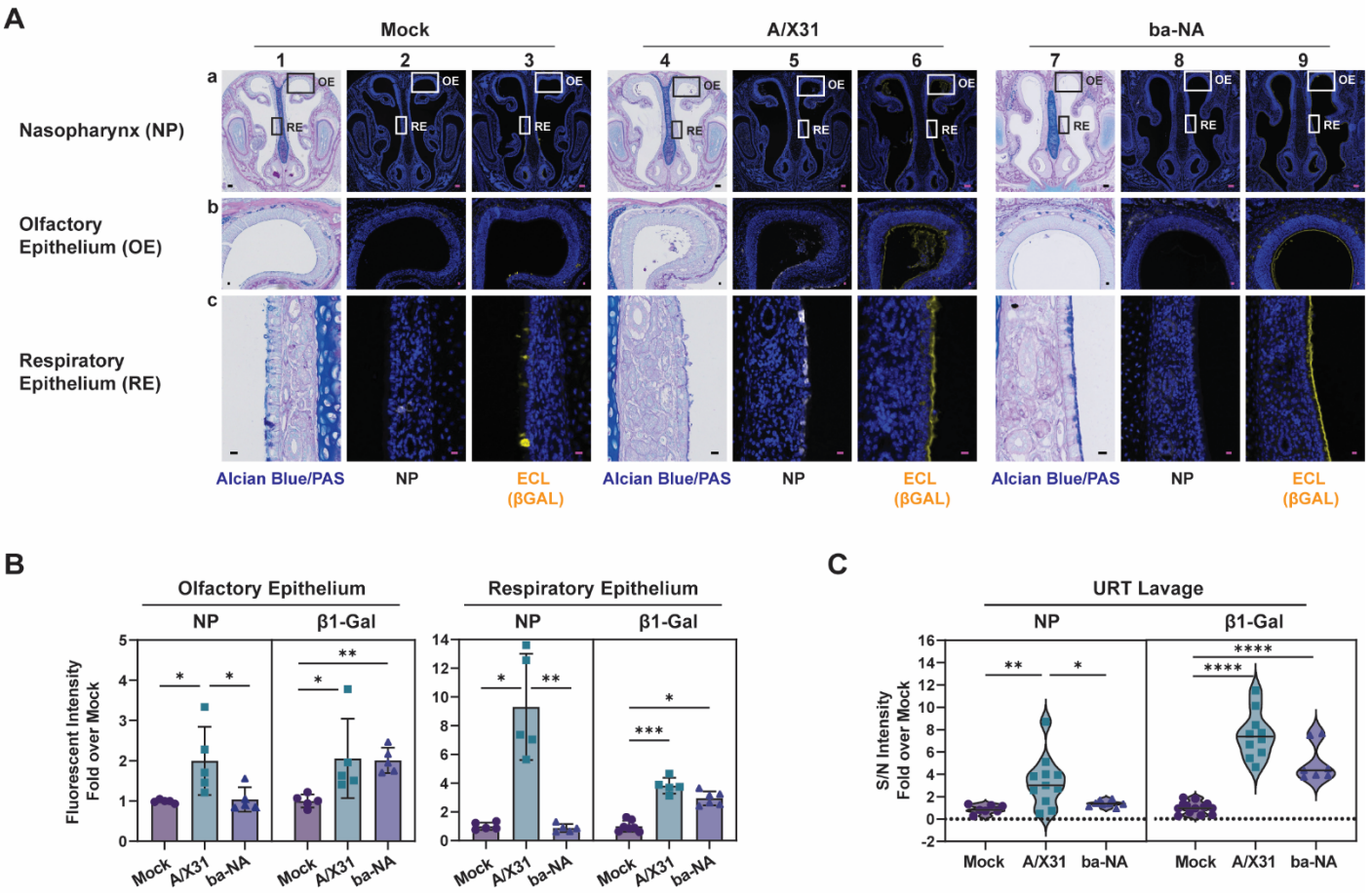

Figure 4. *In vivo* desialylation with broadly-acting neuraminidase.

A. Immunohistochemistry of uninfected, A/X31-infected, and ba-NA-treated infant mice nasopharynx. After sacrifice, heads were fixed with 4% paraformaldehyde, paraffin embedded, sectioned through the nasopharynx, and stained with Influenza anti-NP antibody (white) or conjugated ECL (yellow). Zoomed-in images of the boxed inserts are represented by rows b, and c. Experiments represent at least 2 biological replicates. Infant mice were 4-7 day old; AB/PAS, alcian blue and periodic acid-Schiff stain; NP, influenza nucleoprotein antibody; ECL, *erythrina crystagalli* lectin. **B.** Fluorescent signal from immunohistochemistry (in A) was assessed using ImageJ. Signals for each epithelial compartment was obtained in 5 random locations of at least 2-3 individual mice. Values were normalized to size of the head, and fold induction was calculated over the mock average signal. Bars represent median ± interquartile range. **C.** Mock or ba-NA-treated or A/X31-infected pups were subjected to retrograde URT lavage, and fluid was immunostained with biotinylated-Flu-M antibody or biotinylated-ECL to assess for viral infection or desialylated β-galactose in lavage fluid, respectively. Signals were normalized to membrane background. Median is denoted by a line. **All panels**: Differences among two group medians were analyzed using the Mann-Whitney test, and multiple comparisons was done using the Kruskal-Wallis test. Experiments represent at least 2 biological replicates. Infant mice were 4-7 day old; * ($p < 0.05$), ** ($p < 0.01$), *** ($p < 0.001$), **** ($p < 0.001$). URT, upper respiratory tract; Mock group represents the vehicle-treated (placebo) group; ba-NA group represents the DAS181-treated group. AB/PAS, alcian blue and periodic acid-Schiff stain; NP, Flu-NP antibody stained group, β-gal, ECL, *erythrina crystagalli* lectin-treated group; S/N, signal-to-noise ratio; Dotted line denotes limit of detection.

FIGURE 5

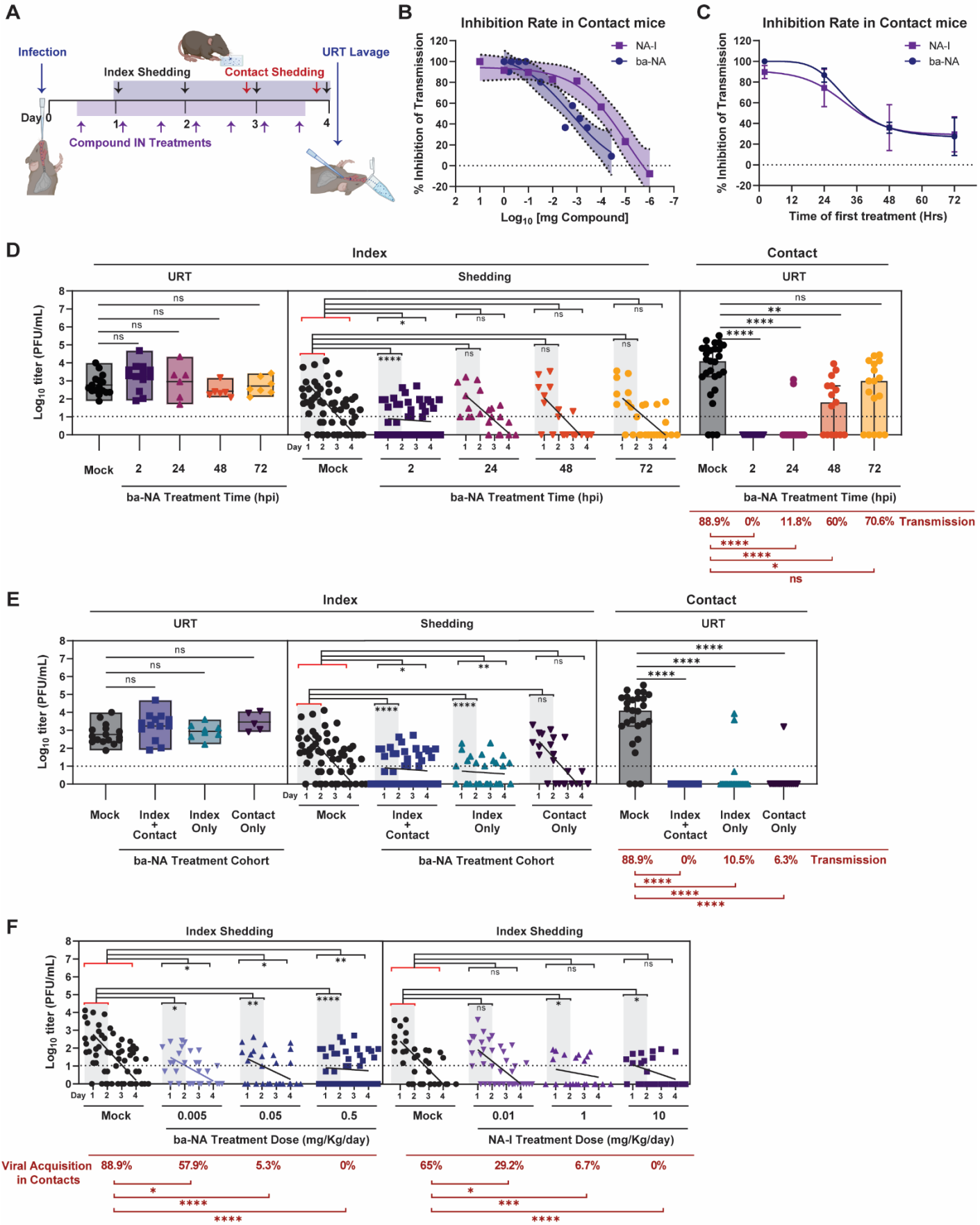
A
Infection
Index Shedding
Contact Shedding
URT Lavage
Day 0
1
2
3
4
Compound IN Treatments
B
Inhibition Rate in Contact mice
NA-I
ba-NA
% Inhibition of Transmission
Log10 [mg Compound]
C
Inhibition Rate in Contact mice
NA-I
ba-NA
% Inhibition of Transmission
Time of first treatment (Hrs)
D
Index
Contact
URT
Shedding
URT
Log10 titer (PFU/mL)
Mock
2
24
48
72
ba-NA Treatment Time (hpi)
88.9%
0%
11.8%
60%
70.6%
Transmission
E
Index
Contact
URT
Shedding
URT
Log10 titer (PFU/mL)
Mock
Index + Contact
Index Only
Contact Only
ba-NA Treatment Cohort
88.9%
0%
10.5%
6.3%
Transmission
F
Index Shedding
Index Shedding
Log10 titer (PFU/mL)
Mock
0.005
0.05
0.5
ba-NA Treatment Dose (mg/Kg/day)
Mock
0.01
1
10
NA-I Treatment Dose (mg/Kg/day)
Viral Acquisition in Contacts
88.9%
57.9%
5.3%
0%
65%
29.2%
6.7%
0%

Figure 5. Broadly-acting neuraminidase inhibits influenza virus transmission *in vivo*.

A. Schematic of compound treatment to block influenza virus transmission. At day 0, pups were infected IN with 300 PFU of A/X-31 (index) and cohoused with uninfected littermates (contact) for 4 days prior to being evaluated for transmission via retrograde URT lavage after sacrifice. Shedding was collected on days 1-4 for index and days 3-4 for contacts by dipping the nostril of each pup into viral media and assessing for infectious virus via plaque assay. IN compound treatment was started 2 hpi and continued once daily for ba-NA (DAS181) or twice daily for NA-I (zanamivir) until end of experiment. **B.** Transmission inhibition rate in contact mice represented as percent (%) inhibition over decreasing compound (ba-NA or NA-I) concentration. % Inhibition was calculated using the following formula: y=100*(1-(y/91.7)) for ba-NA, where 91.7 is the average transmission rate of mock (vehicle-treated) litters, and y=100*(1-(y/65)) for NA-I, where 65 is the average transmission rate of mock (vehicle-treated) litters. Mean transmission is plotted with error bars representing the standard error of the mean (shaded). **C.** Transmission inhibition rate in contact mice represented as percent (%) inhibition over increasing time to compound (inhibitor) treatment. % Inhibition was calculated using the formulas described in (B). Mean transmission is plotted with error bars representing the standard error of the mean. **D.** Transmission inhibition by ba-NA-treatment time is represented by virus titers plotted at each stage of transmission. Left panel (stage 1, index URT replication), middle panel (stage 2, index shedding), right panel (stage 3, contact acquisition). **E.** Transmission inhibition by ba-NA-treatment of individual cohorts is represented by virus titers plotted at each stage of transmission. Left panel (stage 1, index URT replication), middle panel (stage 2, index shedding), right panel (stage 3, contact acquisition). **F.** Shedding titers of A/X31-infected index pups treated with increasing compound (ba-NA or NA-I) concentration. **All panels**: Median is denoted by a line. within box plots and bar graphs ± interquartile range. Simple linear regression was plotted in shedding panels. Differences among multiple group medians were analyzed using the Kruskal-Wallis test. Experiments represent at least 2 biological replicates. Transmission rates were calculated using Fisher's Exact test. Infant mice were 4-7 day old; * ($p < 0.05$), ** ($p < 0.01$), *** ($p < 0.001$), **** ($p < 0.001$). Red brackets in statistical comparisons represent the reference group. URT, upper respiratory tract; PFU, plaque-forming unit; IN, intranasal; Mock group represents the vehicle-treated (placebo) group. Dotted line denotes limit of detection (10 PFU/mL), where indicated; Zero values were set to 1 PFU/mL.

Desialylation of α2,3-SA and α2,6-SA with broadly-acting neuraminidase does not enhance shedding or URT replication of influenza viruses or streptococcus pneumoniae.

Broadly-acting NA functions by depleting SA from the surface of cells, thereby preventing important pathogen interaction with the URT epithelium. This strategy holds great potential for preventing transmission of influenza viruses and other pathogens that rely on SA for infection or pathogenesis. However, there is a theoretical concern that desialylation may have a reverse effect and actually enhance transmission by facilitating the release of progeny virions that remain adhered to SA via the viral hemagglutinin (HA) protein (27-29). To address this concern, we conducted a plaque reduction assay to directly assess the effect of the broadly-acting NA on the phenotype of A/X-

31 plaques. Madin-Darby canine kidney (MDCK) cell monolayers were infected with an equal dose of A/X-31 in each well. After one hour, plaque media containing ba-NA, lectins, or an anti-Flu-nucleoprotein (NP) antibody was overlaid onto the infected cell monolayer. The plates were then incubated at 37°C for 48-72 hours before immunostaining. The formation and size of plaques serve as a measure of the ability of progeny infectious particles to spread to neighboring cells. Results showed that the presence of lectins and the control anti-Flu-NP antibody did not significantly reduce the amount of plaques compared to the mock condition (**Fig.6A**). In contrast, the presence of ba-NA led to a significant reduction in plaque formation compared to the mock condition. This confirms that ba-NA has a direct effect on preventing viral replication and spread, consistent with previous findings from cell-protection assays (24).

To evaluate the preventive effect of ba-NA on infection *in vivo*, we conducted prophylaxis treatment experiments using infant mice. Pups in a litter were pre-treated IN with PBS or ba-NA one day prior to A/X-31 IN challenge with 300 PFUs. After sacrifice at 1 dpi, virus titers in the URT were assessed by analyzing the lavage fluid. Remarkably, pre-treatment with ba-NA led to a significant inhibition of URT viral infection following IN challenge ($P<0.0001$), and in some cases, pups were completely protected from infection (**Fig.6B**). effect on URT viral replication in the presence of ba-NA was also observed when the treatment was administered therapeutically, with virus infection occurring prior to ba-NA treatment by 2 hours and URT replication assessed at 1 dpi. In both prophylaxis and therapeutic scenarios, ba-NA treatment did not enhance virus replication in the URT.

We proceeded to investigate whether ba-NA could enhance the transmission of other influenza virus subtypes that inherently exhibit a low transmission phenotype (LT) (9). Index pups in a litter were infected IN with 300 PFUs of selected viruses, as previously described (**Fig.6C**). To specifically examine the potential effect of ba-NA on enhancing viral shedding, only index pups received daily IN treatment with ba-NA for 4 days, starting at 2 hpi. Daily collection of virus shedding was performed, and intralitter transmission was assessed in contact littermates by measuring virus in retrograde URT lavages at 4 dpi. Viral titers were assessed in mock (black) and ba-NA-treated (blue) groups at the different stages of transmission. The impact of ba-NA treatment on viral replication titers in the URT of index pups (stage 1) varied among viral strains, with some strains displaying greater susceptibility to ba-NA treatment than others (**Fig.6C-1**). Conversely, viral shedding titers from index pups (stage 2) were significantly inhibited across all viral strains tested upon ba-NA treatment (**Fig.6C-2**). Consistently, titers in contact pups were also lower for all viral strains, particularly for those strains exhibiting moderate and high transmission rates in mock-treated pups (**Fig.6C-3**). Notably, there was no enhancement observed in the LT viruses at any stage following ba-NA treatment.

Next, we investigated the impact of ba-NA treatment on the transmission of other respiratory pathogens, specifically focusing on *Streptococcus pneumoniae* (*Spn*). Spn expresses NA on its surface, enabling it to remove SA from host cells and facilitate immune evasion, attachment, and invasion of host cells. This enzyme plays a crucial role in Spn pathogenesis by allowing the bacteria to colonize the URT and cause disease (30). Previous studies have shown that influenza virus NA enhances Spn colonization in tissue culture and mouse lungs (31), and the release of free SA during influenza virus infection, mediated by viral neuraminidase activity, promotes Spn replication (32). To assess whether the supplementation of ba-NA could increase URT Spn density, shedding, and transmission to naïve contact littermates, we employed the infant mouse model of Spn transmission (33). Index pups in a litter were infected with 1000 CFU of Spn in the URT. Only index pups received daily IN treatment with ba-NA for 4 days, starting at 4 dpi. Daily collection of Spn shedding was performed by gently tapping the nares of pups onto bacterial plates 10 times. Intralitter transmission was assessed in contact littermates by measuring Spn levels in retrograde URT lavages at 4 dpi. Compared to the PBS treatment, ba-NA did not enhance URT Spn density, shedding, or transmission. Even when Spn co-infection occurred with A/X-31, where transmission was improved to 75% in the mock treatment group, ba-NA treatment inhibited Spn shedding and transmission regardless (**Fig.6C-purple/green**). These findings suggest that URT desialylation by ba-NA did not result in an increase in Spn bacterial density or shedding. Instead, it is likely that ba-NA deprived the bacteria of an important nutrient, namely SA. this data demonstrates the efficacy of ba-NA in preventing replication, shedding, and transmission of various influenza viruses using an in vivo small animal model. Furthermore, ba-NA also exhibits an important inhibitory role against other respiratory pathogens that interact with URT SA, such as Spn. Importantly, no enhancement of transmission for any pathogen was observed after exogenous desialylation following viral infection in any of the tested conditions in this model.

FIGURE 6

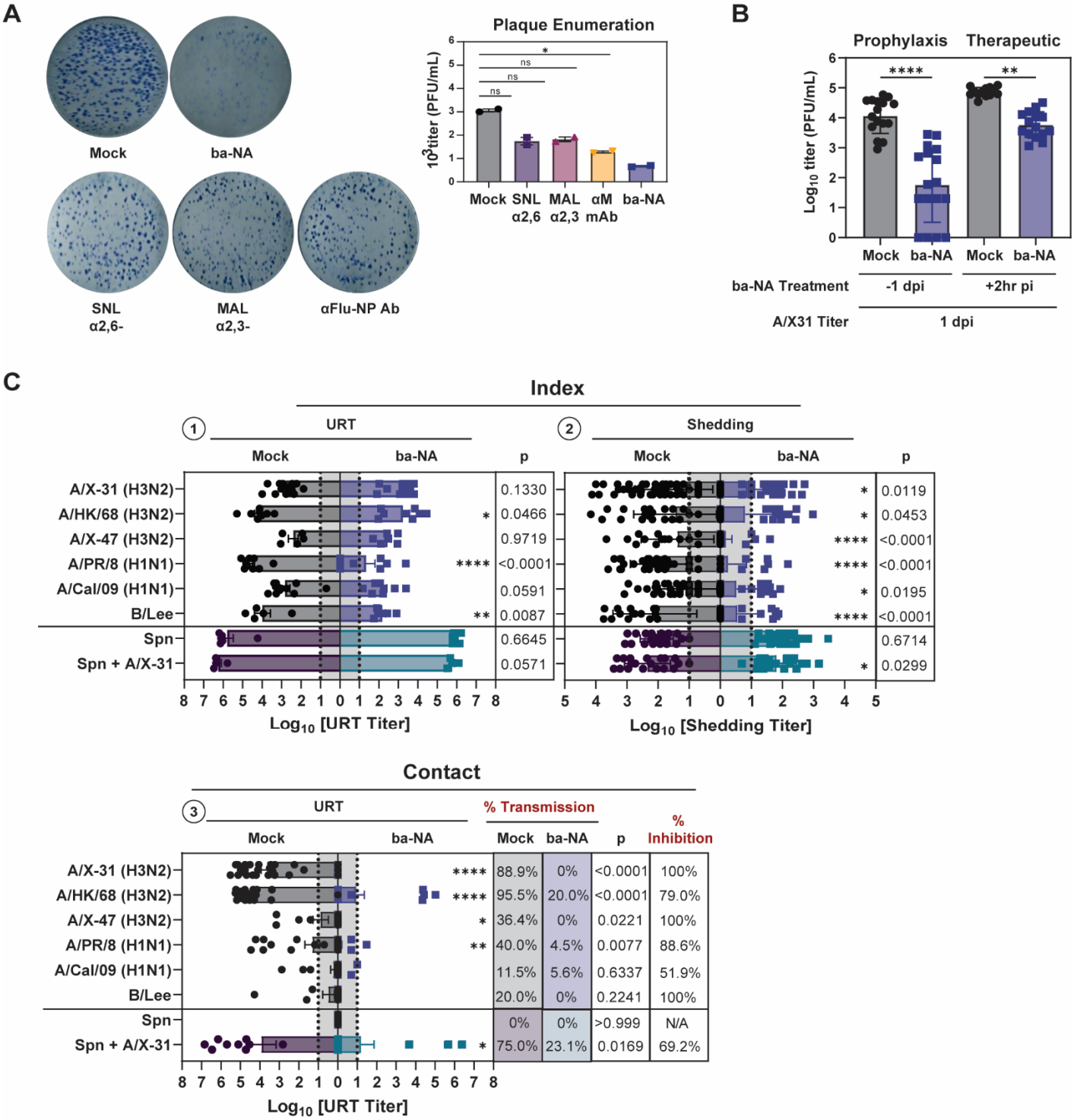

Figure 6. Broadly-acting neuraminidase does not enhance transmission of respiratory pathogens.

A. Plaque reduction assay testing the inhibitory capacity of ba-NA, lectins, and anti-Flu-NP antibody against A/X31. MDCK cells were infected with equal dose of A/X-31 across each condition, and overlayed with agar containing individual compounds at 2mg/mL for 48-72 hr. Cellular monolayer was fixed with 4% paraformaldehyde and then immunostained with Flu-NP antibody. Plaques were enumerated manually. **B.** Prophylaxis and therapeutic capacity of

ba-NA. Pups in a litter were treated with ba-NA 1 day prior or 2 hrs after A/X-31 infection with 300 PFU. Virus titers were assessed at 1 dpi by retrograde URT lavage after sacrifice. **C.** Transmission of multiple influenza virus strains and Spn in the presence or absence of index-treatment with ba-NA. Index pups in a litter were infected IN with 300 PFUs of selected viruses (or 1000 CFU Spn). Only index pups were treated IN daily with ba-NA for 4 days, with the first treatment starting at 2 hpi. Shedding of virus was collected daily and intralitter transmission was assessed in contact littermates by measuring virus from retrograde URT lavages at 4 dpi. Viral (and Spn) titers were assessed in mock (black for virus, purple for Spn) and ba-NA-treated groups (blue for virus or green for Spn) at the different stages of transmission. **All panels**: Differences among two group medians were analyzed using the Mann-Whitney test, and multiple comparisons was done using the Kruskal-Wallis test. Experiments represent at least 2 biological replicates. Infant mice were 4-7 day old; * ($p < 0.05$), ** ($p < 0.01$), *** ($p < 0.001$), **** ($p < 0.001$). URT, upper respiratory tract; PFU, plaque-forming unit; CFU, colony-forming unit; Mock group represents the vehicle-treated (placebo) group; ba-NA group represents the DAS181-treated group; Spn, *Streptococcus pneumoniae*; MDCK, Madin-Darby canine kidney cells; NP, Flu-NP antibody stained group, Dotted line denotes limit of detection.

Discussion

The interaction of influenza virus with the host's sialylated sugars in the URT remains very complex and not well understood. The current understanding of virus tropism and transmission efficiency in humans is heavily dependent on *in vitro* studies categorizing influenza viruses as "avian-like" if they preferentially bind to α2,3-SA or "human-like" if they preferentially bind to α2,6-SA. The SA linkage preference of influenza viruses however, is not sufficient to explain the strain-specific phenotypes observed in the infant mouse model, particularly with respect to transmission. For example, A/Aichi/68 (H3N2), A/Victoria/75 (H3N2) all have preferential binding to α2,6-SA in *in vitro* assays, yet transmission efficiencies in infant mice is 95% and 36%, respectively (21). Furthermore, the recombinant strain A/X-31 which also has preferential binding to α2,6-SA in *in vitro* assays (20), successfully transmits in mice lacking α2,6-SA linkages in the URT. This suggests that some viruses have the capacity to utilize more than one SA linkage during transmission, hence increasing the breadth of their transmission potential.

With the infant mouse model, we can decipher the biology of transmission via successful virus transit through three separate stages: URT replication in infected index (stage 1), shedding of virus from the index (stage 2), and acquisition of virus in naïve contacts (stage 3) (**Fig. 1**). In this study, we focused on understanding the contribution of the URT SA repertoire by leveraging mouse biology, and demonstrate the critical role for the host's sialylated glycoconjugates in shedding and acquisition of influenza viruses *in vivo*.

We demonstrate that both α2,3-SA and α2,6-SA are present in the URT and lungs of infant and adult mice via IHC. Similar to the results in primary mTECs (13), α2,6-SA was also not detected in infant or adult mice tracheas in this study (**Suppl Fig. 1**), but were detected in the URT and lungs (**Fig. 2C**). This implies that some influenza viruses may not require α2,6-SA expression in the trachea to facilitate transmission (binding and elution), which typically happens in the URT. Alternatively, viruses that utilize SA as receptors in general may be more promiscuous in their SA linkage preference than previously thought. This is a significant finding that should be considered in our understanding of influenza virus biology.

Next, we quantified the composition and amount of SA present in the URT of infants and adult mice to address whether variations in expression contributed to the differences in susceptibility to infection between these two age groups. Using two independent methods (IHC and immunoblotting of nasal lavages), we learned that adult mice in general had lower expression of both α2,3-SA and α2,6-SA in the URT compared to infants, which corresponded to their lower index shedding and susceptibility to viral acquisition in contacts (**Fig. 2**). With this in mind, we hypothesized that inhibiting or removing SA moieties in infants would decrease the efficiency of transmission in this age group. Indeed, the efficiency of A/X-31 transmission to naïve contacts was reduced when α2,3-SA and/or α2,6-SA were blocked prophylactically using SA-specific lectins, MAL1 and SNL respectfully. Single α2,6-SA or dual SA blockade were the most effective at inhibiting viral transmission (**Fig. 3**). To address if blocking α2,6-SA was sufficient to block transmission, we acquired a *st6gal1*-KO mouse strain which fails to conjugate terminal α2,6-SA in all tissues, including the URT (**Suppl. Fig. 2**). Surprisingly, like in WT mice, transmission of A/X-31 was very efficient (100%) in this strain, which was inconsistent with the results obtained by blocking α2,6-SA with SNL (37.8% transmission). We hypothesize that α2,6-SA blockade with SNL *in vivo* was perhaps an overestimation of its true inhibitory capacity. SNL is known to be a tetrameric protein composed of four subunits with an estimated combined molecular weight of 140 kDa (34, 35). In contrast MAL are reported to be smaller and exists as a homodimer or heterodimer, with an overall estimated molecular weight of 75 kDa (36). Therefore, it is possible that the increased inhibitory effect observed with prophylactic SNL treatments of contacts is a result of α2,6-SA blockade and associated steric hindrance, given the larger size of this molecule. However, dual blockade using SNL and MAL combination treatments, *st6gal1*-KO and MAL treatment, or removal of both α2,3-SA and α2,6-SA with ba-NA yielded consistent results, such that abrogation of the virus interaction with SA of both α2,3- and α2,6- linkages was necessary and sufficient to inhibit transmission of A/X-31 and other influenza virus subtypes in our model (**Fig. 5 and 6**).

Considering the demonstrated ability of Spn and co-infected viruses to enhance Spn colonization and pathogenesis through NA activity, we were apprehensive that ba-NA inhibitors may have inadvertent impacts on co-colonizing bacterial pathogens. To investigate this, we conducted experiments to evaluate the effects of ba-NA on Spn replication, shedding, and transmission in the presence or absence of co-infection with IAV. Our results indicated that ba-NA treatment significantly reduced Spn shedding in all IAV-infected cohorts. Moreover, none of the Spn cohorts, regardless of co-infection status with IAV, exhibited any enhancement of Spn replication, shedding, or transmission to contacts. These findings extend previous observations showing that ba-NA treatment of IFV -infected mice reduced Spn colonization (37).

In conclusion, our findings from figures 3 and 5 revealed that simultaneous blocking or removal of both α2,3-SA and α2,6-SA significantly reduced viral shedding in index mice. This observation was surprising as the presence of SA is not believed to be necessary for virus shedding from cell surfaces. In contrast, previous studies conducted in tissue culture have demonstrated that exogenous NA promotes viral replication and elution from cells (28). To delve deeper into this discrepancy, we examined the shedding efficiency under two conditions: one where SA was absent (achieved through ba-NA treatment) and another where the interaction between SA and A/X31 was disrupted (using viral NA-I). Our results indicated that shedding was disrupted in a dose-dependent manner in both conditions, suggesting that the production of new influenza virions relies on a sequential interaction between viral HA and NA. Specifically, the presence of SA is required for efficient virion budding and egress through the likely involvement of HA on the virion surface, followed by the cleavage of SA by NA for successful release of viral particles. Further mechanistic investigations are needed to fully explore and test this hypothesis.

It is possible that a therapeutic targeting a host factor may be less susceptible to resistance development compared to targeting viral factors which can lead to the emergence of escape mutants. Therefore, ba-NA have the potential to become the first antiviral agent capable of inhibiting viral shedding when administered directly to the nasal mucosa therapeutically, as well as protecting against viral acquisition when used prophylactically. In summary, ba-NA inhibitors may represent a promising breakthrough in antiviral therapy, with the potential to outsmart viral evolution and revolutionize our approach to preventing and treating viral infections.

Methods

Mice

Wild-type C57BL/6J (strain 000664) was obtained from Jackson Laboratories (Bar Harbor, ME). *st6gal1*-KO mice which lack the enzyme β-galactoside α2,6-sialotransferase 1 (ST6GAL1) was obtained from Joseph T. Y. Lau (Roswell Park Cancer Institute, Buffalo, NY) (22). Breeding was done in-house. Pups were housed with the dam for the duration of all experiments. Animal studies were conducted in accordance with the Guide for the Care and Use of Laboratory Animals (73) and approved by the Institutional Animal Care and Use Committee of NYU Langone Health (assurance no. A3317-01). All procedures followed the Biosafety in Microbiological and Biomedical Laboratories recommendations (74). Genotyping of *st6gal1*-KO mice was done using standard protocols for DNA extraction of ear notch, and performing PCR with the KAPA2G Fast HotStart Genotyping Mix (501965243, Fisher) using the following primers: Fwd (common): CTGAATGGTGGACTGTGG, Rev (*st6gal1*-KO) CATTTTGTGAGCCCCATTAG, Rev (*st6gal1*-WT) TGTTGAAGGGAGAATCTGTG. Expected band sizes are 1200 bp for WT mice and 500b bp for KO mice (22).

Biological Reagents:

Cells: Madin-Darby canine kidney (MDCK) cells were obtained from ATCC, and cultured in Dulbecco's modified Eagle's medium with 10% fetal bovine serum and 1% penicillin-streptomycin. Mycoplasma testing was done monthly.

Viruses: A/X-31 (H3N2) virus (with HA/NA genes from A/Aichi/2/1968 and internal genes from A/Puerto Rico/8/1934) was a gift from Jan Erickson (University of Pennsylvania). Virus sequence was deposited in NCBI GenBank (Accession numbers OQ925911-18).The following reagents were obtained through BEI Resources (NIAID, NIH): A/X-47 (H3N2) (HA/NA genes from A/Victoria/3/1975 and internal genes from A/Puerto Rico/8/1934) (NR-3663), A/Hong Kong/1/1968-2 MA 21-2 (H3N2) (NR-28634), A/Puerto Rico/8/1934 (H1N1) V-301-011-000 (NR-3169), A/California/4/2009 (H1N1) (NR-13659), and B/Lee/1940 V-302-001-000 (NR-3178). IAV and IBV were propagated in 8 to 10-day-old embryonated chicken eggs (Charles River, CT) for 2 days at 37 and 33°C, respectively. Allantoic fluid was then harvested, and subjected to ultracentrifugation (10,000 RPM for 30 minutes at 4C, twice) to clear any debris. Viruses were aliquoted and stored at -80C.

Bacteria: A streptomycin-resistant derivative of capsule type 4 isolate TIGR4 (P2406) was used in this study and cultured on tryptic soy agar (TSA)-streptomycin (200 µg/ml) (33)

Compounds: Broadly-acting neuraminidase (DAS181, Fludase®) was obtained from Ansun BioPharma, Inc (San Diego, CA); Zanamivir (SML0492, Sigma); unconjugated SNL (L-1300-5, Vector Laboratories); biotinylated SNL (B-1305-2, Vector Laboratories); SNL-Cy5 (CL-1305-1, Vector

Laboratories); unconjugated MAL-I (L-1310-5, Vector Laboratories); biotinylated MAL-I (B1315-2, Vector Laboratories); biotinylated ECL (B-1145-5, Vector Laboratories); fluorescein streptavidin (SA-5001-1 Vector Laboratories).

Antibodies: Influenza A virus nucleoprotein antibody, IgG mouse monoclonal (anti-Flu-NP, AA5H, ab20343, Abcam), Biotinylated influenza A virus antibody, IgG polyclonal (biotinylated-anti-Flu, ab20351, Abcam); horseradish peroxidase [HRP]-labeled goat anti-mouse IgG (HRP-anti-mouse IgG, ab205719, Abcam)

Virus infection, shedding, and transmission

Pups in a litter (3 to 7 days of age) were infected (index) with 3µl inoculum without general anesthesia (to avoid direct lung inoculation) by IN instillation of 300 PFU of IAV and returned to the litter at the time of inoculation for the duration of the experiment. Adult mice (8-10 weeks of age) were infected with 10µl inoculum without general anesthesia with 300 PFU of IAV. Shedding of virus was collected by dipping the nares of each mouse into viral medium (PBS plus 0.3% bovine serum albumin [BSA]) daily, and samples were evaluated via plaque assay. Intralitter transmission was assessed in littermates/cagemates (contact) at 4 dpi. Mice were euthanized by CO_2 asphyxiation followed by cardiac puncture, the URT was subjected to a retrograde lavage (flushing of 300 µl PBS from the trachea and collecting through the nares), and samples were used to quantify viral titers (via plaque assay). Ratios of index to contact pups ranged from 1:3 to 1:4.

Compound treatments

Where indicated, pups were IN treated with the following compounds and their vehicles (see biological compound section for ordering information): Lectins were diluted in lectin buffer [sterile water with 10mM HEPES, 0.15M NaCl, 0.1mM CaCl2, 0.08% NaN3], dosed by weight (mg/Kg/day), and treated twice daily. Maximum dose was 10mg/Kg/day; ba-NA [DAS181, Fludase®] was diluted in sterile PBS, dosed by weight (mg/Kg/day), and treated once daily. NA-I [zanamivir, Relenza®] was diluted in sterile water, dosed by weight (mg/Kg/day), and treated twice daily.

Virus growth and quantification

Infectious titers of all stock viruses, and virus present in lavage and shedding fluids obtained from mice were determined by standard plaque assay in MDCK cells in the presence of TPCK (tolylsulfonyl phenylalanyl chloromethyl ketone)-treated trypsin (20233; Thermo Scientific) (75). Briefly, MDCK cell monolayers in 6-well plates, were infected with 200µl inoculum of serially diluted (10-fold) samples. After 45-60 minutes, virus was aspirated and plaque media (2X DMEM/F12 [20233; Thermo Scientific] supplemented with pen/strep, glutamine, HEPES, NaHCO3, 0.4% BSA)

was overlaid onto infected wells and incubated for 48-72 hrs. Plaques were visualized and enumerated manually after 1% crystal violet counter-staining when indicated.

Plaque reduction assay

Monolayers of MDCK cells were infected with equal amounts of A/X-31 virus (~200 PFU/mL/well of a 6-well plate). After 45-60 minutes, virus was aspirated and plaque media containing lectins, DAS181, or anti-Flu-NP antibody diluted at 2mg/mL was overlaid onto infected cells. After 2-3 day incubation at 37C, plates were fixed with 4% paraformaldehyde and agar removed. Plaques were immunostained with 1:1000 anti-Flu-NP primary antibody for 1 hr. Three washes [PBS plus 0.5% milk powder] were done prior to addition of 1:5000 secondary antibody HRP-anti-mouse IgG. After 1hr incubation and three washes, plaques were visualized after addition of TrueBlue HRP substrate (5067428, Fisher) for 1 minute.

Immunostaining of nasal secretions

Lavage fluid from mice were diluted 1:50 in TBS (tris-buffered saline) buffer, and 150 μL was loaded to slots in a blotting apparatus (Minifold II, Schleicher & Schuell) containing pre-wetted 0.2μm nitrocellulose membrane (GE10600094; Amersham Protran). After applying vacuum, membrane was blocked with Carbofree buffer (SP-5040-125, Vector Laboratories) with gentle shaking for 1h at RT followed by incubation with 0.2μg/mL of biotinylated-lectins or biotinylated-anti-Flu primary antibody diluted in TBS-T [TBS plus 0.1% Tween-20] overnight at 4C with gentle shaking. Membrane was then washed 5-6 times with TBS-T for 60 minutes prior to incubation with 1:100000 secondary antibody, streptavidin-HRP conjugate (21130; Pierce) diluted in TBS-T. After incubation (1h at 20°C) and five washes (10 min each) with TBS-T, membrane was developed for 2-5 minutes with 1mL SuperSignal West Femto substrate (34095; Thermo Scientific). Chemiluminescent signal was assessed using ImageJ. TBS-T buffer served as background. A positive control of lavage fluid from A/X-31 infected samples was included on all blots to serve as a normalization value.

Immunohistochemistry

Pups (uninfected, A/X-31-infected, or ba-NA-treated) were euthanized after 2 days as per standard euthanasia protocol. Skin from the heads were gently removed to preserve nasal structures. Heads were decapitated and submerged in PBS at 4°C for a brief wash, followed by fixation in 4% paraformaldehyde for 48-72 h at 4°C without shaking. Heads were then washed in PBS at 4°C with gentle swirling x 20 min, followed by decalcification by fully submerging heads into EDTA solution [0.12M for infants, 0.25M for adults] at 4°C with gentle shaking for 7 days for infants or 21 days for adults. Intact heads were then processed through graded ethanols to xylene and infiltrated with

paraffin in a Leica Peloris automated tissue processor. Five µm paraffin-embedded sections were immunostained on a Leica BondRX automated stainer, according to the manufacturer's instructions. In brief, deparaffinized sections were first incubated with Rodent Block (Biocare, RBM961 L) prior to a 2 hr incubation with lectins (Cy5-SNL (Vector Labs, B-1303 or 5 at dilution 1:50, biotinylated-MAL-I (Vector Labs, B-1315) at a 1:100 dilution, biotinylated-MAL-2 (Vector Labs, B-1265) at a 1:50 dilution, biotinylated-ECL (Thermo, MS-145-B1) at 1:200 dilution, or anti-Flu-NP antibody(Abcam, ab20343) at a 1:500 dilution for 1 hr. Biotinylated lectins were followed by Streptavidin-fluorescein (Vector Labs, SA-5001; 1:50), whereas the anti-Flu antibody was followed by Mouse-on-Mouse HRP-conjugated polymer (Biocare MM620L) and Opal 620 Reagent (Akoya Biosciences, FP1495001T). Slides were counterstained with DAPI and scanned on an Akoya Polaris Vectra imaging system. Images were viewed and prepared with Akoya Phenochart and InForm or OMERO software prior to exporting as TIF files.

Statistical analysis

Microsoft Excel and GraphPad Prism (version 9.4, San Diego, CA) was used for all statistical analyses. Unless otherwise noted, data were analyzed using the Mann-Whitney U test to compare two groups, and the Kruskal-Wallis test with Dunn's post analysis for multiple group comparisons. * ($p < 0.05$), ** ($p < 0.01$), *** ($p < 0.001$), **** ($p < 0.001$)

Data Availability

The authors confirm that data will be made publicly available at the time of publication upon request.

Acknowledgments

We thank Joseph T. Y. Lau for providing *st6gal1*-KO mice, Ansun BioPharma, Inc (Trevor Gale and Stephen Hawley) for providing DAS181 (Fludase®), and the NYU Experimental Pathology Laboratory for their collaboration in this work (Mark Alu, Branka Brukner Dabovic, Shanmugapriya Selvaraj, and Valeria Mezzano). The Experimental Pathology Research Laboratory (RRID:SCR_017928) is partially supported by the Cancer Center Support Grant P30CA016087 at NYU Langone's Laura and Isaac Perlmutter Cancer Center. The original Akoya/PerkinElmer Vectra® imaging system was awarded through the Shared Instrumentation Grant S10 OD021747. Research was supported by the following: NIH/NIAID K08AI141759 to M.B.O., NIH/NIAID R01AI150893 and R37AI038446 to J.N.W., and by NYU Grossman School of Medicine.

References

1. Andrewes CH, Laidlaw PP, Smith W. 1934. The susceptibility of mice to the viruses of human and swine influenza. Lancet 2:859-862.
2. Francis T, Jr. 1934. Transmission of Influenza by a Filterable Virus. Science 80:457-9.
3. Shope RE. 1935. The Infection of Mice with Swine Influenza Virus. J Exp Med 62:561-72.
4. Eaton MD. 1940. Transmission of Epidemic Influenza Virus in Mice by Contact. J Bacteriol 39:229-41.
5. Schulman JL, Kilbourne ED. 1963. Experimental Transmission of Influenza Virus Infection in Mice. I. The Period of Transmissibility. J Exp Med 118:257-66.
6. Edenborough KM, Gilbertson BP, Brown LE. 2012. A mouse model for the study of contact-dependent transmission of influenza A virus and the factors that govern transmissibility. J Virol 86:12544-51.
7. Klinkhammer J, Schnepf D, Ye L, Schwaderlapp M, Gad HH, Hartmann R, Garcin D, Mahlakoiv T, Staeheli P. 2018. IFN-lambda prevents influenza virus spread from the upper airways to the lungs and limits virus transmission. Elife 7.
8. Lowen AC, Mubareka S, Tumpey TM, Garcia-Sastre A, Palese P. 2006. The guinea pig as a transmission model for human influenza viruses. Proc Natl Acad Sci U S A 103:9988-92.
9. Ortigoza MB, Blaser SB, Zafar MA, Hammond AJ, Weiser JN. 2018. An Infant Mouse Model of Influenza Virus Transmission Demonstrates the Role of Virus-Specific Shedding, Humoral Immunity, and Sialidase Expression by Colonizing Streptococcus pneumoniae. mBio 9.
10. Ellstrom P, Jourdain E, Gunnarsson O, Waldenstrom J, Olsen B. 2009. The "human influenza receptor" Neu5Ac alpha2,6Gal is expressed among different taxa of wild birds. Arch Virol 154:1533-7.
11. Eriksson P, Lindskog C, Lorente-Leal V, Waldenstrom J, Gonzalez-Acuna D, Jarhult JD, Lundkvist A, Olsen B, Jourdain E, Ellstrom P. 2019. Attachment Patterns of Human and Avian Influenza Viruses to Trachea and Colon of 26 Bird Species - Support for the Community Concept. Front Microbiol 10:815.
12. Shinya K, Ebina M, Yamada S, Ono M, Kasai N, Kawaoka Y. 2006. Avian flu: influenza virus receptors in the human airway. Nature 440:435-6.
13. Ibricevic A, Pekosz A, Walter MJ, Newby C, Battaile JT, Brown EG, Holtzman MJ, Brody SL. 2006. Influenza virus receptor specificity and cell tropism in mouse and human airway epithelial cells. J Virol 80:7469-80.
14. Glaser L, Conenello G, Paulson J, Palese P. 2007. Effective replication of human influenza viruses in mice lacking a major alpha2,6 sialyltransferase. Virus Res 126:9-18.
15. Ning ZY, Luo MY, Qi WB, Yu B, Jiao PR, Liao M. 2009. Detection of expression of influenza virus receptors in tissues of BALB/c mice by histochemistry. Vet Res Commun 33:895-903.
16. Ivinson K, Deliyannis G, McNabb L, Grollo L, Gilbertson B, Jackson D, Brown LE. 2017. Salivary Blockade Protects the Lower Respiratory Tract of Mice from Lethal Influenza Virus Infection. J Virol 91.
17. Ortigoza MB, Blaser S, Zafar MA, Hammond A, Weiser JN. 2018. An infant mouse model of influenza virus transmission demonstrates the role of virus-specific shedding, humoral immunity, and sialidase expression by colonizing Streptococcus pneumoniae. bioRxiv doi:10.1101/456665.
18. Kamiki H, Murakami S, Nishikaze T, Hiono T, Igarashi M, Furuse Y, Matsugo H, Ishida H, Katayama M, Sekine W, Muraki Y, Takahashi M, Takenaka-Uema A, Horimoto T. 2022. Influenza A Virus Agnostic Receptor Tropism Revealed Using a Novel Biological System with Terminal Sialic Acid Knockout Cells. J Virol doi:10.1128/jvi.00416-22:e0041622.
19. Yang H, Carney PJ, Chang JC, Guo Z, Villanueva JM, Stevens J. 2015. Structure and receptor binding preferences of recombinant human A(H3N2) virus hemagglutinins. Virology 477:18-31.
20. Childs RA, Palma AS, Wharton S, Matrosovich T, Liu Y, Chai W, Campanero-Rhodes MA, Zhang Y, Eickmann M, Kiso M, Hay A, Matrosovich M, Feizi T. 2009. Receptor-binding specificity of pandemic influenza A (H1N1) 2009 virus determined by carbohydrate microarray. Nat Biotechnol 27:797-9.
21. Peng W, de Vries RP, Grant OC, Thompson AJ, McBride R, Tsogtbaatar B, Lee PS, Razi N, Wilson IA, Woods RJ, Paulson JC. 2017. Recent H3N2 Viruses Have Evolved Specificity for Extended, Branched Human-type Receptors, Conferring Potential for Increased Avidity. Cell Host Microbe 21:23-34.
22. Nasirikenari M, Veillon L, Collins CC, Azadi P, Lau JTY. 2014. Remodeling of marrow hematopoietic stem and progenitor cells by non-self ST6Gal-1 sialyltransferase. J Biol Chem 289:7178-7189.

23. Oswald DM, Lehoux SD, Zhou JY, Glendenning LM, Cummings RD, Cobb BA. 2022. ST6Gal1 in plasma is dispensable for IgG sialylation. Glycobiology doi:10.1093/glycob/cwac039.
24. Malakhov MP, Aschenbrenner LM, Smee DF, Wandersee MK, Sidwell RW, Gubareva LV, Mishin VP, Hayden FG, Kim DH, Ing A, Campbell ER, Yu M, Fang F. 2006. Sialidase fusion protein as a novel broad-spectrum inhibitor of influenza virus infection. Antimicrob Agents Chemother 50:1470-9.
25. Chemaly RF, Marty FM, Wolfe CR, Lawrence SJ, Dadwal S, Soave R, Farthing J, Hawley S, Montanez P, Hwang J, Ho JH, Lewis S, Wang G, Boeckh M. 2021. DAS181 Treatment of Severe Lower Respiratory Tract Parainfluenza Virus Infection in Immunocompromised Patients: A Phase 2 Randomized, Placebo-Controlled Study. Clin Infect Dis 73:e773-e781.
26. Krammer F, Smith GJD, Fouchier RAM, Peiris M, Kedzierska K, Doherty PC, Palese P, Shaw ML, Treanor J, Webster RG, Garcia-Sastre A. 2018. Influenza. Nat Rev Dis Primers 4:3.
27. Nishikawa T, Shimizu K, Tanaka T, Kuroda K, Takayama T, Yamamoto T, Hanada N, Hamada Y. 2012. Bacterial neuraminidase rescues influenza virus replication from inhibition by a neuraminidase inhibitor. PLoS One 7:e45371.
28. Kamio N, Imai K, Shimizu K, Cueno ME, Tamura M, Saito Y, Ochiai K. 2015. Neuraminidase-producing oral mitis group streptococci potentially contribute to influenza viral infection and reduction in antiviral efficacy of zanamivir. Cell Mol Life Sci 72:357-66.
29. Zhang H. 2008. Concerns of using sialidase fusion protein as an experimental drug to combat seasonal and pandemic influenza. J Antimicrob Chemother 62:219-23.
30. Hammond AJ, Binsker U, Aggarwal SD, Ortigoza MB, Loomis C, Weiser JN. 2021. Neuraminidase B controls neuraminidase A-dependent mucus production and evasion. PLoS Pathog 17:e1009158.
31. Peltola VT, Murti KG, McCullers JA. 2005. Influenza virus neuraminidase contributes to secondary bacterial pneumonia. J Infect Dis 192:249-57.
32. Siegel SJ, Roche AM, Weiser JN. 2014. Influenza promotes pneumococcal growth during coinfection by providing host sialylated substrates as a nutrient source. Cell Host Microbe 16:55-67.
33. Zafar MA, Kono M, Wang Y, Zangari T, Weiser JN. 2016. Infant Mouse Model for the Study of Shedding and Transmission during Streptococcus pneumoniae Monoinfection. Infect Immun 84:2714-22.
34. Broekaert WF, Nsimba-Lubaki M, Peeters B, Peumans WJ. 1984. A lectin from elder (Sambucus nigra L.) bark. Biochem J 221:163-9.
35. Shibuya N, Goldstein IJ, Broekaert WF, Nsimba-Lubaki M, Peeters B, Peumans WJ. 1987. The elderberry (Sambucus nigra L.) bark lectin recognizes the Neu5Ac(alpha 2-6)Gal/GalNAc sequence. J Biol Chem 262:1596-601.
36. Yamamoto K, Konami Y, Irimura T. 1997. Sialic acid-binding motif of Maackia amurensis lectins. J Biochem 121:756-61.
37. Hedlund M, Aschenbrenner LM, Jensen K, Larson JL, Fang F. 2010. Sialidase-based anti-influenza virus therapy protects against secondary pneumococcal infection. J Infect Dis 201:1007-15.